Proceedings of the 2006 IEEE
International Conference on Control Applications
Munich, Germany, October 4-6, 2006

Sideslip angle, lateral tire force and road friction estimation in simulations and experiments

Guillaume Baffet, Ali Charara and Joanny Stéphant

***Abstract*— Transversal tire forces and sideslip angle are essential data for improving vehicle safety, handling, steerability, comfort and performance. This paper proposes and compares four observers designed to calculate vehicle sideslip angle and lateral tire forces. The different observers are derived from the Extended Kalman filter (EKF), the single-track model, and use different on tire-force models. The first three tire-force models are the linear model, the Burckhardt model and the Pacejka model. The remaining tire-force model, the "linear adaptive" model, is proposed in this paper in order to construct an adaptive observer. The "linear adaptive" model is based on the linear model, but with an additional variable used to correct wheel cornering stiffness errors. The paper describes models and observers, along with a road-friction identification method. Observers are first compared in a simulation context using a professional vehicle simulator. Subsequently, observers are applied to real experimental data acquired on the Heudiasyc Laboratory car.**

I. INTRODUCTION

Knowledge of vehicle-dynamic and environment variables (road friction and profile) is an essential part of safety improvement, in particular for braking and trajectory-control systems. Accurate data about tire forces and sideslip angle lead to a better evaluation of road friction and a better definition of a vehicle's possible trajectories, and make possible the development of a diagnostic tool able to evaluate the potential risks of accidents related to poor adherence or dangerous maneuvers.

One problem is that forces and sideslip angle are difficult to measure directly, and the cost of currently available sensors is prohibitive for ordinary cars[1]. The solution proposed in the present study is to estimate the unmeasurable variables from the Extended Kalman filter (EKF) [5] and available standard sensors.

A similar study concerning the estimation of sideslip angle has already been undertaken [11]. Other studies ([9], [8]) present valid tire-force observers, but involving wheel-torque measurements[2]. In this study, all observers (O_{rl}, O_{rb}, O_{rp}, O_{la}) require measurements of lateral acceleration, yaw rate and steering angle (Fig. 1). This work extends a previous study [1] which presents and compares O_{rl}, O_{rb} and O_{rp} EKF for dry-road friction conditions.

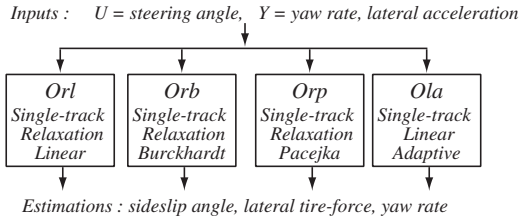

Fig. 1. Vehicle state observers O_{rl}, O_{rb}, O_{rp}, O_{la}.

This study presents the adaptive observer Ola and evaluates the robustness of the four observers with tire-road friction changes. Observers and friction identification methods are first evaluated with respect to data obtained from a vehicle-dynamic simulation program (CALLAS). The simulations performed include normal and critical driving situations, and a wide range of road frictions and velocities were simulated. Next, observers are evaluated in relation to sideslip angle in critical driving situations. Finally, an observability analysis is performed for all tests.

The different notations are listed in Appendix VIII.

II. VEHICLE-ROAD MODELS

A. Single-Track Model

The single-track model, developed by Segel [10], is currently used to describe transversal vehicle-dynamic behavior. In this study, longitudinal and vertical movements are ignored, and so no longitudinal acceleration and roll are taken into account. The simplified single-track model is :

$$\begin{aligned}\dot{\beta} &= (F_{y1}\cos(\delta-\beta)+F_{y2}\cos(\beta))/(mV_g)-\dot{\psi},\\ \ddot{\psi} &= (L_1F_{y1}\cos(\delta)-L_2F_{y2})/I_z.\end{aligned} \quad (1)$$

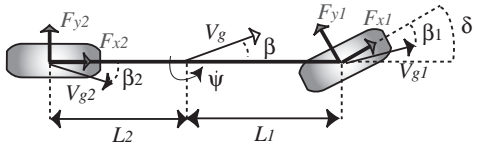

Fig. 2. Single-track model.

B. Tire-Road Friction

Tire-road friction is defined as the ratio of the frictional force acting in the wheel plane to the vertical wheel-ground

This work was supported by the PREDIT program, and with the help of SERA-CD (http://www.sera-cd.com).

Guillaume Baffet and Ali Charara are at the Heudiasyc Laboratory (UMR CNRS 6599), Université de Technologie de Compiègne, Centre de recherche Royallieu, BP20529 - 60205 Compiègne, France, gbaffet@hds.utc.fr, acharara@hds.utc.fr

Joanny Stéphant is with XLIM/DMI/MOD equip, ENSIL, Parc d'Ester Technopole, 87068 Limoges, France, stephant@ensil.unilim.fr

[1]A dynamometric wheel cost around 100 K€and a sideslip angle sensor costs approximately 15 K€.

[2]Wheel-torque sensors cost around 35 K€.

contact force :

$$\mu(g) = (F_x(g)^2 + F_y(g)^2)^{1/2}/F_z. \quad (2)$$

Friction can be calculated using Burckhardt's method [4] :

$$\mu(g) = c_{e1}(1 - \exp(-c_{e2}g)) - c_{e3}g, \quad (3)$$

where the parameters c_{e1}, c_{e2} and c_{e3} are given for various roads in [4] (Fig. 3). The wheel slip g is the geometrical sum of the longitudinal slip g_l and the sideslip g_t :

$$g = (g_l^2 + g_t^2)^{1/2}, \quad g_l = (v_w - rw)/v_w, \quad g_t = \tan(\beta). \quad (4)$$

Ignoring longitudinal slip, and assuming a small sideslip angle, (2) and (3) become :

$$\mu(\beta) = c_{e1}(1 - \exp(-c_{e2}, |\beta|)) - c_{e3}|\beta| = |F_y(\beta)|/F_z. \quad (5)$$

C. Lateral tire-force models

The model of tire-road contact forces is complex because a wide variety of parameters including environmental factors and pneumatic properties impact the tire-road contact interface. Many tire-force models have been proposed, from empirical methods (Pacejka model [7]) to analytical methods (LuGre model [3]). This study uses four tire-force models (the nominal linear model, the adaptive linear model, the Pacejka model and the Burckhardt model, Fig. 4) corresponding to four observers (O_{rl}, O_{la}, O_{rp}, O_{rb}). The linear and the Pacejka model are selected because these models are references as the most commonly used tire-force models. The Burckhardt model is also selected because it comprises few parameters, and it analytic expression is simple.

D. Relaxation Model

When vehicle sideslip angle changes, a lateral tire force is created with a time lag. This transient behavior of tires can be formulated using a relaxation length σ_i. The relaxation length is the distance covered by the tire while the tire force is kicking in. Using the relaxation model presented in [2], transversal forces can be written as :

$$\dot{F_{yi}} = \frac{V_g}{\sigma_i}[-F_{yi} + \overline{F_{yi,n}}], \qquad i = 1,2, \quad n = 1,2,3, \quad (6)$$

where $\overline{F_{yi,n}}$ is calculated from a reference tire-force model ($n = 1,2,3$ respectively for the linear, Burckhardt and Pacejka models).

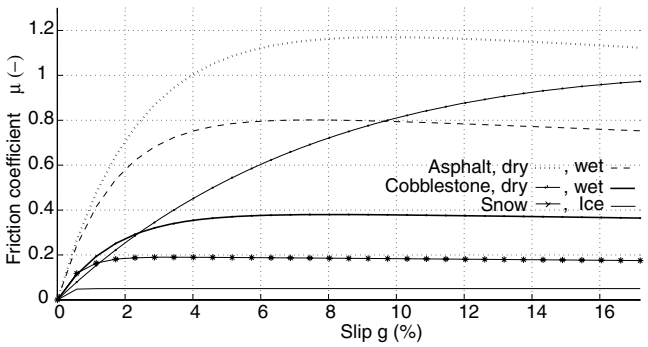

Fig. 3. Friction coefficient characteristics (Burckhardt model).

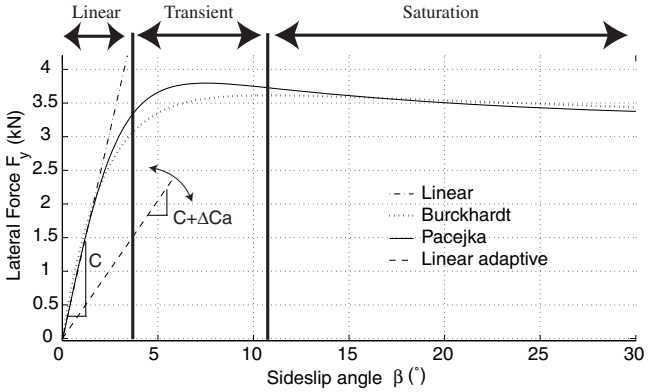

Fig. 4. Lateral pneumatic forces. Linear, Burckhardt, Pacejka and linear adaptive models.

E. Reference Tire-Force models

As shown in Fig 4, there exist three distinct stages of vehicle handling behaviors (the linear, transient and saturation stages). In the first stage, lateral tire forces are linear with respect to sideslip angle. The second and third stages, nonlinear, occur when the vehicle approaches the physical limit of adhesion. The lateral tire force is calculated in the linear model as:

$$\overline{F_{yi,1}}(\beta_i) = C_i\beta_i. \quad (7)$$

This study also uses two nonlinear models: the Burckhardt and Pacejka models. The Burckhardt model is used in the simplified form based on (5) :

$$\overline{F_{yi,2}}(\beta_i) = sign(\beta_i)F_{zi}\mu(\beta_i). \quad (8)$$

The tire-force model proposed by Pacejka [7], often called "the magic Formula", results from parameter identification of experimentally-obtained characteristics. Using this model, lateral tire force may be calculated as

$$\begin{aligned} \overline{F_{yi,3}}(\beta_i) &= D\sin[C\arctan(\Phi(\beta_i + S_h))] + S_v, \\ \Phi(\beta_i) &= B\beta_i - E(B\beta_i - \arctan(B\beta_i)), \end{aligned} \quad (9)$$

where parameters B, C, D, E, s_v and s_h are a function of the wheel load, slip angle, slip ratio and camber. The coefficient D represents the maximum value of the characteristic. The coefficients B and C allow the slope and the shape of the curve to be adjusted. The coefficient E allows control of the X-coordinate (sideslip angle) for which the maximum value of the curve is reached. The parameters S_h and S_v are offsets of the X-coordinate (sideslip angle) and Y-coordinate (lateral tire force) respectively. In this study, the parameters of Pacejka were assumed constant, and set to dry-road values (without Callas parameter identification).

F. Linear Adaptive Model

This study proposes an tire-force model which take into account road friction variation: the linear adaptive model. When road friction changes, or when the nonlinear pneumatic domain is reached, "real" wheel cornering stiffness varies. The linear adaptive model takes into account this

variation via the readjustment variable of wheel cornering stiffness ΔC_{ai} :

$$\overline{F_{yi,4}}(\beta_i) = (C_i + \Delta C_{ai})\beta_i. \tag{10}$$

The variable ΔC_{ai} is estimated as a state in the observer Ola.

III. EKF OBSERVERS

State and input vectors, evolution and measurement equations for the different EKF are :

- for $Orl(n=1,(7))$, $Orb(n=2,(8))$, $Orp(n=3,(9))$:

$$[X_1,X_2,X_3,X_4] = [\beta, \dot{\psi}, F_{y1}, F_{y2}], \quad [U] = [\delta],$$
$$\begin{cases} \dot{X_1} = (X_3\cos(U-X_1) + X_4\cos(X_1))/(mV_g) - X_2, \\ \dot{X_2} = (L_1X_3\cos(U) - L_2X_4)/I_z, \\ \dot{X_3} = (V_g/\sigma_1)(-X_3 + \overline{F_{y1,n}}(\beta_1)), \\ \dot{X_4} = (V_g/\sigma_2)(-X_4 + \overline{F_{y2,n}}(\beta_2)), \end{cases} \tag{11}$$

$$[Y_1,Y_2] = [\dot{\psi}, \gamma_y],$$
$$\begin{cases} Y_1 = X_2, \\ Y_2 = (X_3\cos(U) + X_4)/m, \end{cases} \tag{12}$$

- for $Ola(n=4)$:

$$[X_1,X_2,X_3,X_4] = [\beta, \dot{\psi}, \Delta c_{a1}, \Delta c_{a2}], \quad [U] = [\delta],$$
$$\begin{cases} \dot{X_1} = [\beta_1(C_1+X_3)\cos(U-X_1) + \\ \qquad \beta_2(C_2+X_4)\cos(X_1)]/mV_g - X_2, \\ \dot{X_2} = (L_1(C_1+X_3)\beta_1\cos(U) - L_2(C_2+X_4)\beta_2)/I_z, \\ \dot{X_3} = 0, \\ \dot{X_4} = 0, \end{cases} \tag{13}$$

$$[Y_1,Y_2] = [\dot{\psi}, \gamma_y],$$
$$\begin{cases} Y_1 = X_2, \\ Y_2 = ((C_1+X_3)\beta_1\cos(U) + (C_2+X_4)\beta_2)/m, \end{cases} \tag{14}$$

where rear and front sideslip angles are calculated as :

$$\beta_1 = U - X_1 - L_1X_2/V_g, \qquad \beta_2 = -X_1 + L_2X_2/V_g. \tag{15}$$

IV. SIMULATION RESULTS, COMPARISON WITH CALLAS SOFTWARE

The CALLAS program, developed by SERA-CD, is a vehicle-dynamic simulator, which takes into account numerous factors including vertical suspension dynamics, tires, engine model, kinematics, elasto-kinematics, tire adhesion, and aerodynamics. The observers O_{rl}, O_{rb}, O_{rp} and O_{la} are compared using lateral-dynamic data obtained from CALLAS. The trajectory analyzed is a double lane change (DLC) (Fig. 5), at two different speeds ($40km/h$, $90km/h$), and four different road frictions corresponding to a dry ($\mu = 1$), snow-covered ($\mu = 0.3$) and icy road surface ($\mu = 0.15, 0.05$). During tests, the parameters of the tire-force models were assumed constant, and set to dry-road values. The normalized error ε_z for an estimation z is calculated as

$$\varepsilon_z = 100(\|z - z_{measure}\|)/(\max\|z_{measure}\|). \tag{16}$$

Fig. 6 presents the simulation path and vehicle velocity for the different speeds ($40km/h$, $90km/h$) and road frictions (1, 0.3, 0.15, 0.05). When the speed is $40km/h$, the virtual driver ensures a successful DLC, even when road friction decreases

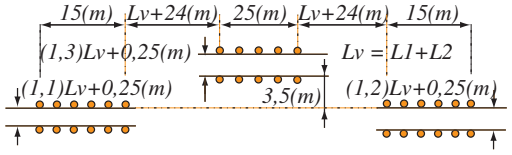

Fig. 5. Double lane change (DLC).

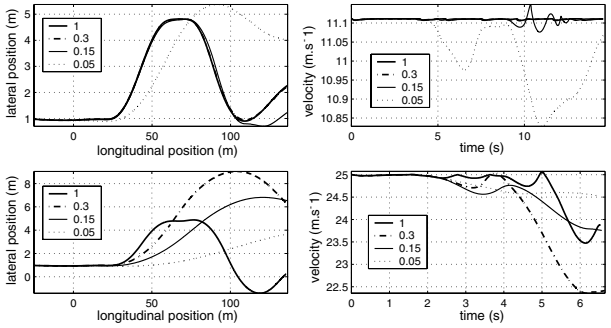

Fig. 6. Path and vehicle speed - 40, 90 km/h - $\mu = 1, 0.3, 0.15, 0.05$.

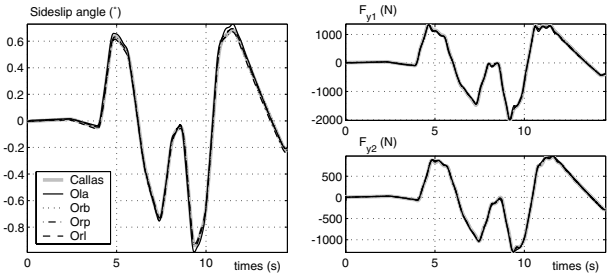

Fig. 7. Sideslip angles and lateral tire forces, $40km/h, \mu = 1$

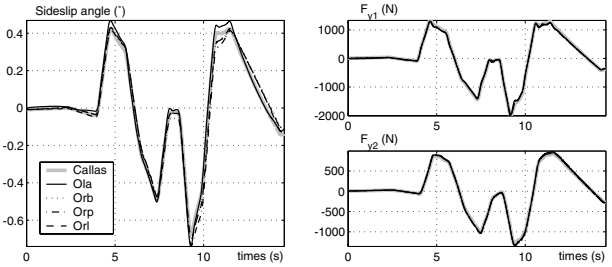

Fig. 8. Sideslip angles and lateral tire forces, $40km/h, \mu = 0.3$

to 0.3. At less than 0.3 the vehicle deviates from the DLC. When the vehicle speed is $90km/h$ and road friction $\mu = 1$, the vehicle accomplishes three quarters of the DLC but leaves it at the end of the maneuver. During the ($90km/h$, $\mu = 0.3$) test, the vehicle leaves the DLC at the first left turn. For the last two tests ($90km/h$, $\mu = 0.15, 0.05$), the vehicle fails to complete the first turn and finishes the maneuver facing the wrong way. Vehicle velocity remains constant for the ($40km/h$, $\mu = 1, 0.3$) tests. For critical tests the simulator decreases vehicle speed, which contravenes the assumption of constant speed, section II-A).

Fig. 7 to 14 present sideslip angle and front and rear lateral tire forces obtained using the different observers in

TABLE I

SIMULATION RESULTS : MAXIMUM ABSOLUTE VALUES, NORMALIZED MEAN ERRORS FOR SIDESLIP ANGLE AND LATERAL FORCES.

$V(km/h)$	40	40	40	90	90	90
$\mu(-)$	$\beta(^o)$	$F_{y1}(N)$	$F_{y2}(N)$	$\beta(^o)$	$F_{y1}(N)$	$F_{y2}(N)$
1	0.9	2015	1291	14.5^o	8539	8040
0.3	0.6	1987	1159	30.4	2836	2464
0.15	4.2	1435	5090	42.2	1382	1191
0.05	24.9	470	396	10.8	467	391

a) Maximum absolute values (simulation)

$V(km/h)$		40	40	40	90	90	90
$\mu(-)$	(%)	ε_β	$\varepsilon_{F_{y1}}$	$\varepsilon_{F_{y2}}$	ε_β	$\varepsilon_{F_{y1}}$	$\varepsilon_{F_{y2}}$
1	O_{rl}	**0.5**	***0.4***	***0.4***	2.3	9.8	6.2
	O_{rb}	**0.5**	***0.5***	***0.6***	0.9	2.9	1.5
	O_{rp}	**1.4**	***0.5***	***0.6***	0.9	2.9	1.5
	O_{la}	**1.7**	***1.2***	***1.0***	1.4	3.6	2.7
0.3	O_{rl}	**2.7**	***1.0***	***1.4***	9.3	123.2	103.6
	O_{rb}	**2.9**	***1.4***	***1.9***	1.1	12.8	7.4
	O_{rp}	**3.5**	***1.2***	***1.6***	1.5	13.0	8.7
	O_{la}	**2.7**	***1.2***	***0.9***	1.3	14.2	3.3
0.15	O_{rl}	7.1	14.9	16.1	5.4	272.0	254.6
	O_{rb}	1.3	5.2	5.7	0.2	18.4	18.1
	O_{rp}	2.6	5.0	5.9	0.5	18.3	21.3
	O_{la}	1.6	2.9	1.9	0.2	16.1	3.2
0.05	O_{rl}	17.2	*470.5*	*425.3*	36.2	*750.5*	*699.3*
	O_{rb}	0.6	49.5	46.4	0.6	77.4	84.3
	O_{rp}	1.1	49.1	51.5	2.0	78.0	96.5
	O_{la}	0.8	21.8	2.7	0.2	21.1	5.7

b) Normalized mean errors (simulation)

relation to CALLAS measurements. Table I(a) gives the maximum values for sideslip angle and lateral tire forces for the different tests. The normalized mean errors of the observers are shown in table I(b). In normal driving condition (Fig. 7, 8), the different observers are accurate with respect to sideslip angle (mean errors less than **5%**). As regards lateral tire forces, good approximations are obtained from the different observers (mean errors less than ***2%***).

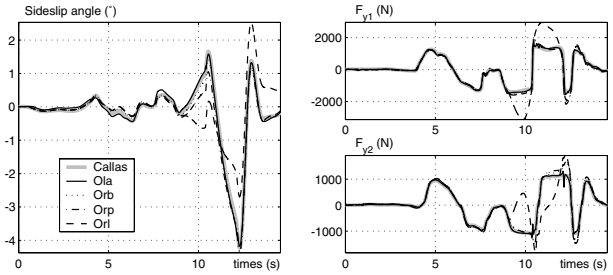

Fig. 9. Sideslip angles and lateral tire forces, $40km/h, \mu = 0.15$

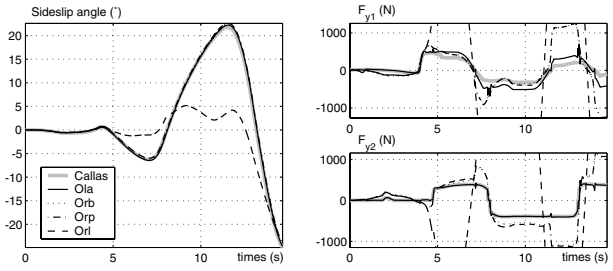

Fig. 10. Sideslip angles and lateral tire forces, $40km/h, \mu = 0.05$

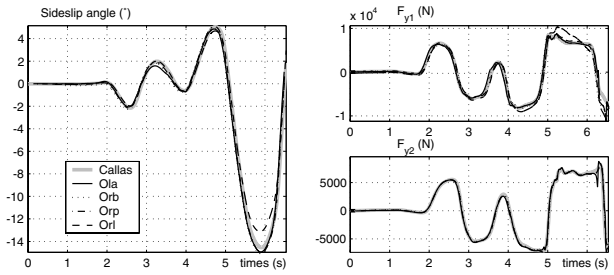

Fig. 11. Sideslip angles and lateral tire forces, $90km/h, \mu = 1$

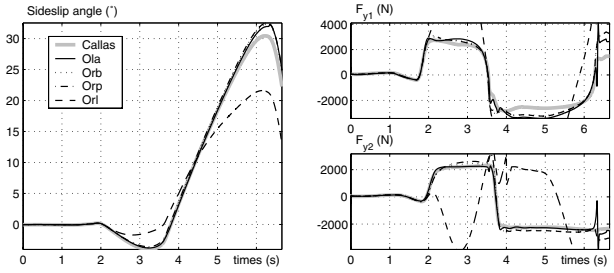

Fig. 12. Sideslip angles and lateral tire forces, $90km/h, \mu = 0.3$

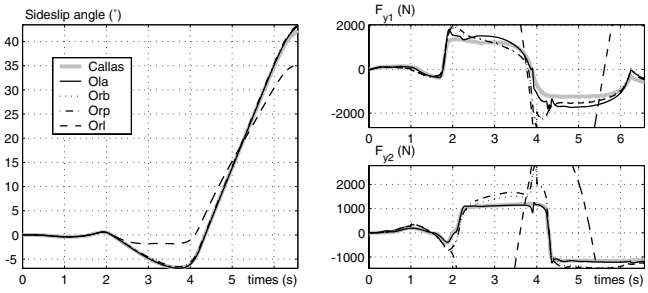

Fig. 13. Sideslip angles and lateral tire forces, $90km/h, \mu = 0.15$

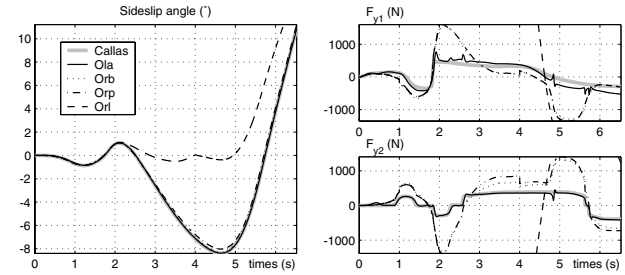

Fig. 14. Sideslip angles and lateral tire forces, $90km/h, \mu = 0.05$

In critical driving conditions (Fig. 9-14) it is apparent that results are significantly different. The curves for the *Orl* observer are incomplete, because errors are very large (mean force errors more than *400%* when $\mu = 0.05$). The principal explanation is that linear models do not take into account the saturation of lateral tire forces when sideslip angle is large. The Burckhardt and Pacejka observers (*Orb*, *Orp*) give similar results: they also produce high lateral force errors for the ($40km/h$, $\mu = 0.15, 0.05$) and ($90km/h$, $\mu = 0.3, 0.15, 0.05$) tests. The Burckhardt and Pacejka model parameters are not readjusted, since *Orb* and *Orp* are not robust with respect to high road friction variations. The *Ola*

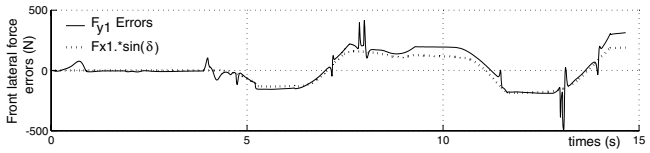

Fig. 15. Front lateral tire force errors (*Ola*), in comparison with the lateral component of F_{x1}, 40 km/h, $\mu = 0.05$.

observer's rear lateral force curves are close to CALLAS (mean errors less than 6%). However, this observer produces significant errors in the front lateral forces for the ($40km/h$, $\mu = 0.05$) and ($90km/h$, $\mu = 0.3, 0.15, 0.05$) tests. This is due to the longitudinal dynamic. Because of speed variations the simplification of longitudinal forces in the single-track model is not valid. This implies that the lateral component of the front longitudinal tire force is not negligible, and consequently this error is found in the estimate of the front lateral tire force. This is illustrated for the ($40km/h$, $\mu = 0.05$) test in Fig. 15.

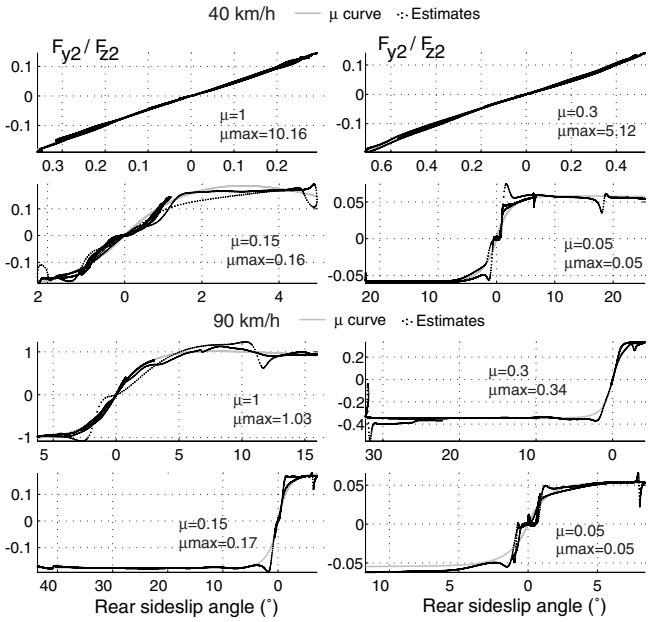

Fig. 16. Normalized rear lateral forces vs rear sideslip angle estimations of *Ola*. Estimated friction curves.

A. Road Friction Characteristics

The *Ola* sideslip angle and rear lateral force estimations are used to identify tire-road friction characteristics. These characteristics are calculated using the Burckhardt model (5). Coefficients c_{e1}, c_{e2}, c_{e3} are obtained by minimizing the following criterion using a Quasi-Newton method :

$$J = [((C_2 + \Delta C_{a2})\beta_2)/F_{z2} - (c_{e1}(1 - \exp(-c_{e2}\|\beta_2\|)) - c_{e3}\|\beta_2\|)], \quad (17)$$

where $(F_{y2}, \beta_2, F_{z2})$ are obtained from *Ola*. Fig. 16 presents - normalized rear lateral force estimations (F_{y2}/F_{z2}) in comparison with identified tire-road friction characteristics, - maxima of estimated characteristics (μ_{max}).

For the first two tests ($40km/h, \mu = 1, 0.3$) value ranges are narrow, so estimated curves are false and the maxima $(10.16, 5.12)$ are not representative of road friction. For the other tests, estimated curves show interesting results : the maxima match simulated road friction $(1, 0.3, 0.15, 0.05)$. Results show that when lateral vehicle dynamics are small (sideslip angle lower than 4^o), there are no sufficiently significant values to identify tire-road friction curves. Conversely, when sideslip angle is higher than 4^o, friction indicators give a good approximation of road friction.

TABLE II

SIDESLIP ANGLE MAXIMAL MEASURES (ABSOLUTE VALUES), NORMALIZED MEAN ERRORS (EXPERIMENT).

	$\max \|\beta_2\|$	O_{rl}	O_{rb}	O_{rp}	O_{la}
DLC	8.9^o	3.9%	2.3%	2.5%	2.9%
Slalom	13.3^o	3.5%	1.6%	1.9%	2.5%

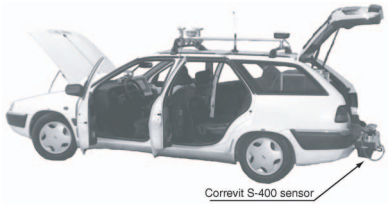

Fig. 17. HEUDIASYC Laboratory experimental vehicle : STRADA.

V. EXPERIMENTAL RESULTS - STRADA

STRADA is the Heudiasyc Laboratory's test vehicle (see Fig. 17), a Citroën Xantia equipped with a number of sensors (GPS, accelerometer, odometer, gyrometer, steering angle and Correvit S-400). STRADA is not equipped with dynamometric wheels, and consequently the lateral forces are not measured. The Correvit S-400 is a non-contact optical sensor mounted at the rear of STRADA. This sensor gives a validation measure of vehicle sideslip.

This study used two experimental hard-test data sets obtained during previous work [11]. The vehicle trajectories and the acceleration diagrams are shown in Fig. 18. In the first hard test the vehicle moved in slalom at an approximate velocity of 80 km/h. In the second hard test the vehicle performed a

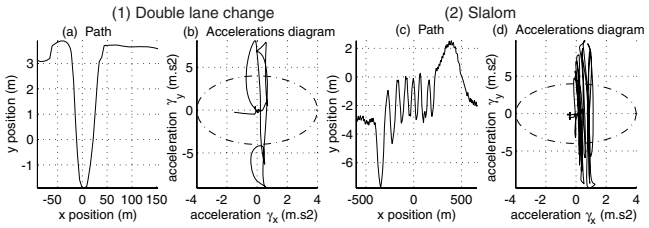

Fig. 18. Path and Accelerations, Slalom and double lane change (experiment).

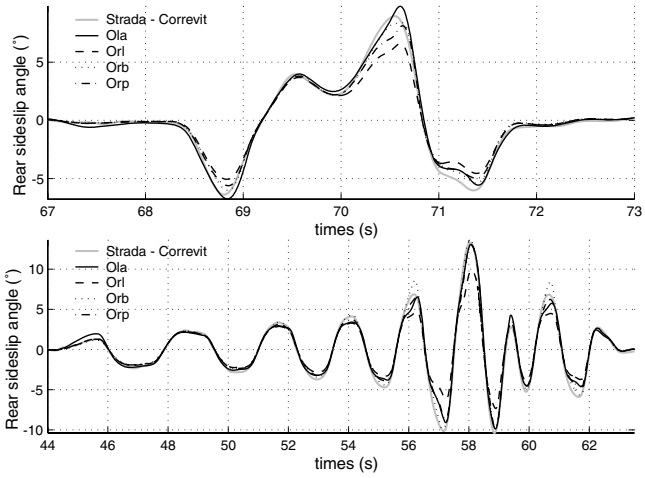

Fig. 19. Rear sideslip angle experimental estimations.

double lane change at 53 km/h. The vehicle's positions were obtained using GPS. Acceleration diagrams (fig. 18(b,d)) show that large lateral acceleration ranges were obtained (above 0.4g). Longitudinal accelerations are not negligible, and consequently the assumption of the simplified one-track model ($F_{x1} = 0$) is not valid.

Table II presents maximum absolute values and normalized mean errors for sideslip angle for the two tests. Fig. 19 presents sideslip angle estimations. The results from *Orb*, *Orp*, *Orl* and *Ola* give good approximations of rear sideslip angles (mean errors less then 4%), in spite of high lateral loads and critical driving maneuvers. Observers O_{rb}, O_{rp} and O_{la} are more effective than O_{rl} for hard vehicle maneuvers. The explanation may be that the linear model is not adapted to represent tire-force saturation, so sideslip angle is underestimated. Observer errors may also be due to neglected effects : normal load variations, roll and longitudinal movements.

VI. OBSERVABILITY ANALYSIS

The observability function was calculated under lateral acceleration and yaw rate measures, using a lie derivative [6]. Ranks of all observability functions were 4 (state dimension) along experimental and simulation trajectories, so systems O_{rl}, O_{rb}, O_{rp} and O_{la} were locally observable.

VII. CONCLUSIONS AND FUTURE WORK

This study deals with four sideslip angle and lateral tire-force observers, and a road friction indicator. The differences between the observers reside in in their different tire-force models.

In simulation, all observers are satisfactory in normal driving conditions. When road friction is low and speed high, the nonlinear observers give good approximations of sideslip angle. Lateral force results depend significantly of the observer used : *Orl* is not robust with nonlinear tire-force dynamics, and *Orb* and *Orp* are not robust with low road friction. Observer *Ola* gives good approximations of rear lateral tire forces. This result justifies the use of an adaptive tire-force model to take into account road friction changes. When longitudinal acceleration is not negligible, the assumption made by the single-track model is false, which implies that observers need to have better model.

The *Ola* estimations are used to identify road friction curves. The road friction indicator yields good results when the lateral dynamic is sufficiently large (sideslip angle more than 4^o). Future studies will improve vehicle/road models in order to widen validity domains for observers. Subsequent vehicle/road models will take into account longitudinal roll and vertical dynamics.

VIII. APPENDIX - NOTATIONS

L_1, L_2 Center of gravity to front, rear, axle distances (m)
m, I_z Vehicle mass (Kg), Yaw moment of inertia ($Kg.m^{-2}$)
r, δ Wheel radius (m), Steering angle (rad)
v_w, w Longitudinal wheel speed ($m.s^{-1}$), Angular wheel velocity ($rad.s^{-1}$)
$V_{g,g1,g2}$ Center of gravity, front, rear, vehicle speed ($m.s^{-1}$)
$\dot{\psi}$, μ Yaw rate ($rad.s^{-1}$), Road friction ($-$)
$g_{,l,t}$ Global, longitudinal, sideslip ($-$)
$\beta_{,1,2}$ Center of gravity, front, rear, sideslip angles (rad)
$\gamma_{x,y}$ Longitudinal, lateral, accelerations ($m.s^{-2}$)
$F_{x,y,z,1,2}$ Longitudinal, lateral, vertical, rear, front, forces (N)
$\sigma_{1,2}$ Front, rear, wheel relaxation length (m)
$C_{1,2}$, $\Delta C_{a1,2}$ Front, rear, adaptive stiffness ($N.rad^{-1}$)
X, U, Y State, input, measure, vectors $\in R^4, R^1, R^3$
$O_{rl,rb,rp,la}$ Linear, Burckhardt, Pacejka, linear adaptive, EKF

REFERENCES

[1] G. Baffet, J. Stéphant, A. Charara, "Evaluation d'observateurs pour l'estimation des efforts latéraux et de la dérive d'un véhicule", *in Proc. Journées Doctorales et Nationales du GDR MACS*, Lyon, France, 2005.

[2] P. Bolzern, F. Cheli, G. Falciola and F. Resta, Estimation of the nonlinear suspension tyre cornering forces from experimental road test data, *Vehicle system dynamics*, vol. 31, 1999, pp 23-34.

[3] C. Canudas-De-Wit, P. Tsiotras, E. Velenis, M. Basset, G. Gissinger, Dynamic friction models for road/tire longitudinal interaction, *Vehicle System Dynamics*, vol. 39, 2003, pp 189-226.

[4] U. Kiencke and L. Nielsen, *Automotive control system*, Springer, 2000.

[5] S. G. Mohinder and P. A. Angus, *Kalman filtering theory and practice*, Prentice hall, 1993.

[6] H. Nijmeijer and A. J. Van der Schaft, *Nonlinear Dynamical Control Systems*, Springer-Verlag, 1990.

[7] H.B. Pacejka and E. Bakker, "The magic formula tyre model", *Proc. 1st Int. colloq. on tyre models for vehicle dynamics analysis*, 1991, pp. 1-18.

[8] A. Rabhi, N.K M'Sirdi, N. Zbiri, Y. Delanne, "Modélisation pour l'estimation de l'état et des forces d'interaction Véhicule-Route", *in Proc. Conférence internationale francophone d'automatique (CIFA2004)*, Douz, Tunisie, 2004.

[9] L. Ray, "Nonlinear Tire Force Estimation and Road Friction Identification : Simulation and Experiments", *Automatica*, vol. 33, no. 10, 1997, pp 1819-1833.

[10] M.L. Segel, "Theorical prediction and experimental substantiation of the response of the automobile to steering control", *Proc. automobile division of the institut of mechanical engineers*, vol. 7, 1956, pp 310-330.

[11] J. Stéphant, *Contribution l'étude et à la validation expérimentale d'observateurs appliqués à la dynamique du véhicule*, Université de Technologie de Compiègne, 2004, December.